

Kinematics of Wheeled Robots

Professor Vijay Kumar
School of Engineering and Applied Science
University of Pennsylvania
June 23, 2020

1 Introduction

In these notes, we will develop the notation and a mathematical model for the geometry and configuration space for wheeled mobile robots and develop a kinematic model for control. scope of this discussion will be limited, for the most part, to differential-drive, planar robots. The extension to self driving cars is quite straightforward.

2 Configuration space and constraints

A planar rigid body has three degrees of freedom. Its position and orientation can be described by three coordinates (x, y, θ) in some reference frame. While $(x, y) \in R^2$, technically θ_i belongs to a subset of R . This is because it is an angle and only takes values in $[0, 2\pi)$ with the values 0 and 2π being identified. This is sometimes denoted as the circle, S^1 . Thus, the configuration space for a single rigid body in the plane is called the *special Euclidean group* in two-dimensions and is denoted by $SE(2)$ [3]:

$$SE(2) = R \times R \times S^1.$$

The configuration space of N planar rigid bodies is:

$$\mathcal{C} = \{X | X \in SE(2) \times SE(2) \times \dots \times SE(2), X = [x_1, y_1, \theta_1, x_2, y_2, \theta_2, \dots, x_N, y_N, \theta_N]\}$$

In a system of two or more particles (rigid bodies), unconstrained motion is simply not possible. To see this consider the simplest possible system involving two particles on a straight line or two frictionless beads sliding on a smooth, taut wire. Since the particles cannot cross each other, there is a constraint on the positions of the two particles. This constraint is an *inequality* constraint.

Similarly, consider a robot (a rigid body) moving in an environment with a fixed obstacle (another rigid body). As shown in Figure 1, the configuration space can be divided into legal configurations that avoid penetration of the robot with the obstacle and illegal configurations. The figure (bottom left) also shows the boundary of the set of configurations $\{x, y, \theta\}$ that result in collisions. Clearly, one can conceptualize the obstacle-free space or the *free space* as the set of configurations that satisfy a given set of inequalities[1].

2.1 Holonomic constraints

We will now turn our attention from inequalities to constraint equalities. Consider a system of N planar rigid bodies. We have already seen that there is a $3N$ -dimensional configuration space associated with the system. However, when there are one or more configuration constraints (as in the case of planar kinematic chains) not all of the $3N$ variables describing the system configuration are independent. We have seen that the minimum number of variables (also called coordinates) to completely specify the configuration (position of every particle) of a system is called the number of degrees of freedom for that system. Thus if there are m independent configuration constraints, the number of degrees of freedom n is given by:

$$n = 3N - m$$

Constraints on the position of a system of particles (as in the examples with kinematic chains) are called *holonomic constraints*. The positions of the particles are constrained by holonomic equations. The system is constrained to move in a subset of the $3N$ -dimensional configuration space. For example, if you take a single rigid body that has a three dimensional configuration space and

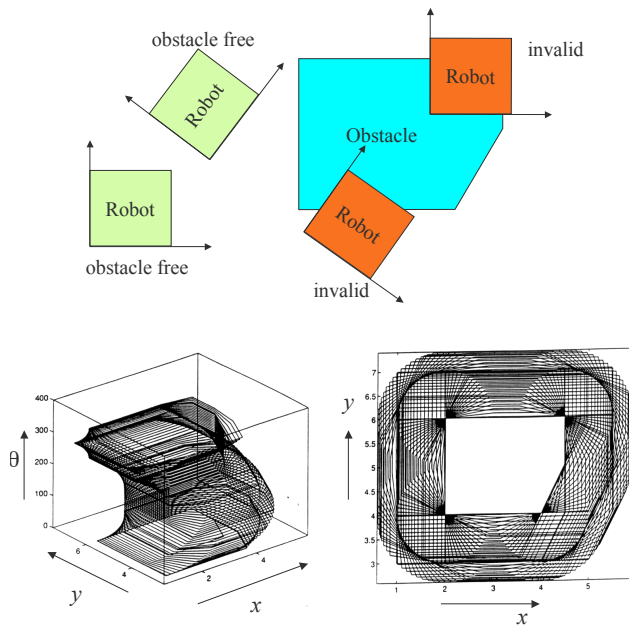


Figure 1: The presence of an obstacle divides the configuration space into free space and the set of invalid configurations (top). The set of invalid configurations in three dimensional space is shown on the bottom left — the projection of this solid on the $x - y$ plane is shown on the bottom right.

force it to pivot about a fixed point, you introduce two constraints and force it to remain in a one-dimensional subset of the configuration space.

2.2 Nonholonomic constraints

In contrast to holonomic constraints in which the positions of the particles are constrained, we may have constraints in which the velocities of the particles are constrained but the positions are not. As an example, consider the constraint called the *knife-edge constraint* illustrated by the skate edge in Figure 3. The rigid body can be described by the coordinates of a reference point C that is the (single) point of contact on the plane (x, y) and the angle (θ) between the longitudinal axes and the x -axis. Since the skate cannot slide in a lateral

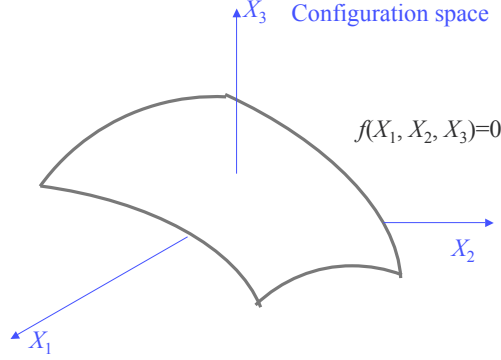


Figure 2: A single constraint in a three-dimensional configuration space forces the resulting two degree-of-freedom system to evolve on a two-dimensional surfaces in the configuration space

direction, the velocity of the point C must be along the longitudinal axis (shown by the vector \mathbf{e}_f). In other words, the velocity of the point C in the lateral direction (\mathbf{e}_l) must be zero. Let us formalize this with equations.

The position and orientation or the *pose* of a robot with a knife-edge constraint as shown in Figure 3 is given by a 3×1 vector:

$$q = \begin{bmatrix} x \\ y \\ \theta \end{bmatrix}$$

Differentiating this equation gives us the velocity:

$$\dot{q} = \begin{bmatrix} \dot{x} \\ \dot{y} \\ \dot{\theta} \end{bmatrix}$$

The velocity of the point C is the 2×1 vector:

$$\mathbf{v}_C = \begin{bmatrix} \dot{x} \\ \dot{y} \end{bmatrix}$$

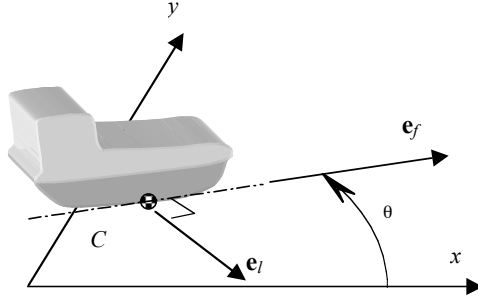


Figure 3: The position of the skate in the plane is described by three coordinates. Thus its configuration space is R^3 or $R^2 \times S^1$. But its velocity can only be along a direction prescribed by Equation (4). Thus the rate of change of the three position coordinates is constrained.

and the vectors \mathbf{e}_f and \mathbf{e}_l are:

$$\mathbf{e}_f = \begin{bmatrix} \cos \theta \\ \sin \theta \end{bmatrix}, \quad \mathbf{e}_l = \begin{bmatrix} \sin \theta \\ -\cos \theta \end{bmatrix}.$$

The longitudinal component of velocity or the component of \mathbf{v}_C along \mathbf{u} , denoted by v_f :

$$v_f = \mathbf{v}_C^T \mathbf{e}_f = \dot{x} \cos \theta + \dot{y} \sin \theta \quad (1)$$

while the lateral component of velocity is:

$$v_l = \mathbf{v}_C^T \mathbf{e}_l = \dot{x} \sin \theta - \dot{y} \cos \theta \quad (2)$$

If there is no slip in the lateral direction, we get the constraint equation $v_l = 0$ or:

$$\dot{x} \sin \theta - \dot{y} \cos \theta = 0 \quad (3)$$

Or in differential form after rearranging terms:

$$dy = \tan \theta \, dx \quad (4)$$

You should try to verify that Equation (4) cannot be integrated to obtain a constraint on x , y , and θ . Rather this equation simply constrains the velocities

and not the positions. Such non integrable velocity constraints as the one in Eq. (3) are called *nonholonomic* constraints.

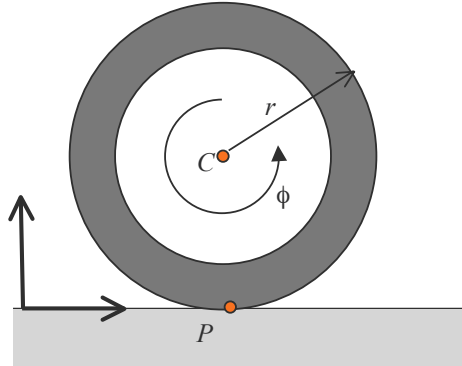


Figure 4: The velocity of the point of contact (P) on a wheel rolling on a stationary surface is zero[5].

2.3 Rolling constraints

You cannot assume all velocity constraints are non integrable. Indeed, it is possible to differentiate any position constraint to obtain a velocity constraint that can be integrated back to the position constraint. Figure 4 provides a pertinent example of a non trivial velocity constraint that can be integrated. Consider the rolling wheel with a point of contact P with the (stationary) ground. Because it is rolling, the velocity of the point P is zero. Suppose the wheel rolls along the y axis on the $y - z$ plane given by $x = 0$. The velocity

of the point C can be obtained from the vector equation ¹:

$$\begin{aligned}
\mathbf{v}_C &= \mathbf{v}_P + \omega \times \overrightarrow{PC} \\
&= \dot{\phi} \hat{\mathbf{i}} \times r \hat{\mathbf{k}} \\
&= -r \dot{\phi} \hat{\mathbf{j}}
\end{aligned} \tag{5}$$

If we were to denote the coordinates of the center of the wheel by (x_C, y_C, z_C) , we can write the equations:

$$\begin{bmatrix} \dot{x}_C \\ \dot{y}_C \\ \dot{z}_C \end{bmatrix} = \begin{bmatrix} 0 \\ -r \dot{\phi} \\ 0 \end{bmatrix} \tag{6}$$

which integrates to:

$$\begin{bmatrix} x_C(t) \\ y_C(t) \\ z_C(t) \end{bmatrix} = \begin{bmatrix} 0 \\ -r \int_0^t \dot{\phi} d\tau \\ r \end{bmatrix} \tag{7}$$

Given the history of forward wheel rotation, we can integrate to get the position (x_C, y_C, z_C) . Thus, the velocity constraints in Equation (6) are holonomic.

3 Kinematics of a Differential Drive Wheeled Robot

Mobile robots for operation on flat terrain have several simplifying features that make them easier to model than real-world trucks or passenger cars. In particular, many robots have two independently-driven, coaxial wheels. An example of such a robot is the SCARAB differential drive robot[2]. The speed difference between both wheels results in a rotation (θ) of the vehicle about the center of the axle while the wheels act in concert to produce motion in the forward or reverse direction along the x_r axis. Second, these robots are

¹If we fix a reference frame to the wheel at the point C , the velocity of the point P is given by the velocity of the origin, \mathbf{v}_C , the angular velocity ω and the position vector \overrightarrow{CP} :
 $\mathbf{v}_P = \mathbf{v}_C + \omega \times \overrightarrow{CP}$

two-dimensional and lack suspensions. In cars, the suspension compensates for vertical motion caused by the cars dynamics at high speeds. Mobile robots operate at relatively low speeds and we assume vertical motion is absent.

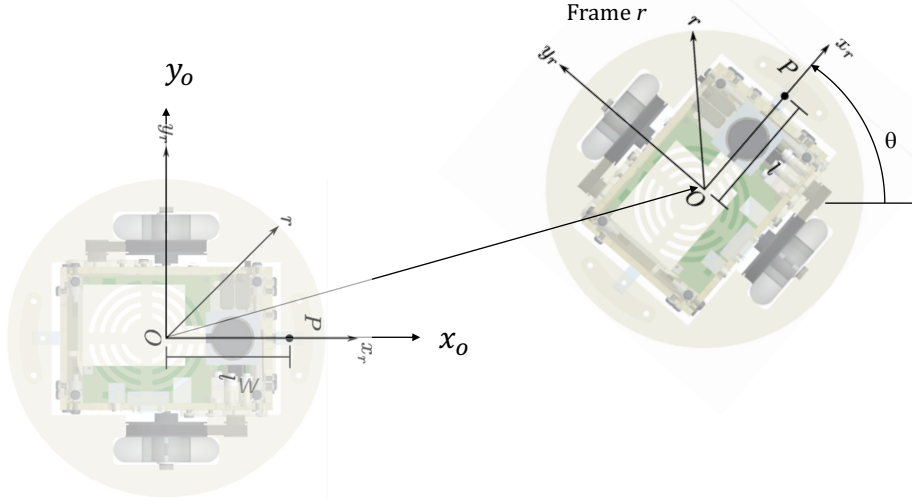


Figure 5: A top view of the SCARAB differential drive robot[2]. The robot-fixed reference frame, r , can be describe with the respect to frame 0 using the orientation θ and a translation vector o_0o_r .

Figure 6 shows two possible schematics for designs of differential drive robots. In both cases the kinematics is determined by the axle and the wheel radii. Denote the centers of the wheels by C_1 and C_2 respectively, and let their radius be r . Let the axle width or the length of the vector $\overrightarrow{C_1C_2}$ be d . Let (x_i, y_i, z_i) denote the position of center C_i and let ϕ_i denote the wheel speed of the i th wheel. And let the component of speed in the longitudinal direction (see Figure 3) be given by $v_{f,i}$. According to Equation (6):

$$\begin{aligned} v_{f,i} &= -r\dot{\phi}_i \\ v_{l,i} &= 0 \end{aligned} \tag{8}$$

From Equation (1) we get

$$v_{f,i} = \dot{x}_i \cos \theta + \dot{y}_i \sin \theta \tag{9}$$

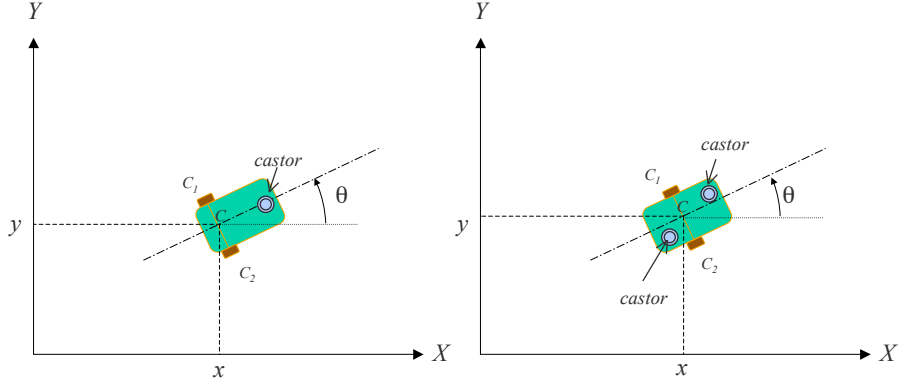


Figure 6: Two possible configurations for differential drive robots. The castors serve to support the weight of the vehicle and under ideal conditions do not affect the kinematics of the robot.

and from Equation (2), we have:

$$0 = \dot{x}_i \sin \theta - \dot{y}_i \cos \theta \quad (10)$$

Note that we are measuring ϕ_i in a counterclockwise direction from one (arbitrarily chosen) side of the mobile robot as shown in Figure 7.

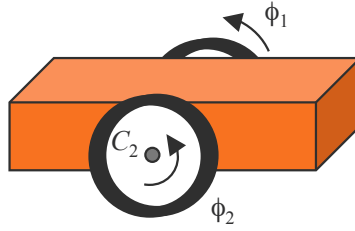


Figure 7: The wheel angles ϕ_i are taken to be positive in a counterclockwise direction from one (arbitrarily chosen) side of the mobile robot.

Now consider the coordinates of the center of the axle (x, y) which is clearly

half way between C_1 and C_2 :

$$x = \frac{x_1 + x_2}{2} \quad y = \frac{y_1 + y_2}{2}.$$

The velocity of the point C is given by:

$$\mathbf{v}_C = \begin{bmatrix} \dot{x} \\ \dot{y} \end{bmatrix} = \begin{bmatrix} \frac{\dot{x}_1 + \dot{x}_2}{2} \\ \frac{\dot{y}_1 + \dot{y}_2}{2} \end{bmatrix} \quad (11)$$

The forward speed or the velocity component in the longitudinal direction can be obtained by projecting along \mathbf{e}_l :

$$\begin{aligned} v_f &= \mathbf{e}_f^T \mathbf{v}_C = \dot{x} \cos \theta + \dot{y} \sin \theta \\ &= \frac{\dot{x}_1 \cos \theta + \dot{y}_1 \sin \theta}{2} + \frac{\dot{x}_2 \cos \theta + \dot{y}_2 \sin \theta}{2} \\ &= \frac{v_{f,1} + v_{f,2}}{2} \\ &= -\frac{r\dot{\phi}_1 + r\dot{\phi}_2}{2} \end{aligned} \quad (12)$$

Now if we consider the two points C_1 and C_2 which are rigidly attached to the axle and the mobile robot, the velocities of these two points are related by the equation:

$$\mathbf{v}_{C_2} = \mathbf{v}_{C_1} + \dot{\theta} \hat{\mathbf{k}} \times \overrightarrow{C_1 C_2} \quad (13)$$

where

$$\mathbf{v}_{C_1} = v_{f,1} \mathbf{e}_f, \quad \mathbf{v}_{C_2} = v_{f,2} \mathbf{e}_f.$$

From the above equation we can write:

$$-r\dot{\phi}_2 \mathbf{e}_f = -r\dot{\phi}_1 \mathbf{e}_f + \dot{\theta} \hat{\mathbf{k}} \times d \mathbf{e}_l.$$

If we write the components along \mathbf{e} , we get:

$$-r\dot{\phi}_2 = -r\dot{\phi}_1 + d\dot{\theta} \quad (14)$$

Thus, we have the two equations that relate the velocity of the mobile robot to the velocities of the wheels:

$$v_f = -\frac{r\dot{\phi}_1 + r\dot{\phi}_2}{2} \quad (15)$$

$$\dot{\theta} = \frac{r\dot{\phi}_1 - r\dot{\phi}_2}{d} \quad (16)$$

4 Forward and Inverse Kinematics

In a differential drive wheeled robot, the wheel angles, $q = (\phi_l, \phi_r)$, take the place of joint angles in a robot arm. The task or Cartesian coordinates are given by:

$$X = \begin{bmatrix} x \\ y \\ \theta \end{bmatrix} \quad (17)$$

where (x, y) are the coordinates of the center, O , in Figure 5, the midpoint of the axle of the differential drive.

The Jacobian for the robot can be obtained

$$\dot{X} = \begin{bmatrix} \frac{r}{2} \cos \theta & \frac{r}{2} \cos \theta \\ \frac{r}{2} \sin \theta & \frac{r}{2} \sin \theta \\ -\frac{r}{d} & \frac{r}{d} \end{bmatrix} \begin{bmatrix} \dot{\phi}_r \\ \dot{\phi}_l \end{bmatrix} \quad (18)$$

where $\phi_l = \phi_1$ and $\phi_r = \phi_2$ in Figure 7. We can write this as:

$$\dot{X} = H\dot{q} \quad (19)$$

where

$$H = \begin{bmatrix} \frac{r}{2} \cos \theta & \frac{r}{2} \cos \theta \\ \frac{r}{2} \sin \theta & \frac{r}{2} \sin \theta \\ -\frac{r}{d} & \frac{r}{d} \end{bmatrix},$$

and $\dot{q}_1 = \dot{\phi}_r$, $\dot{q}_2 = \dot{\phi}_l$. While H maps joint rates into the robot's Cartesian velocities, it is not invertible in its present form. First, the matrix is not square.

If we only want to consider the x and y velocities, we can write:

$$\begin{bmatrix} \dot{x} \\ \dot{y} \end{bmatrix} = \begin{bmatrix} \frac{r}{2} \cos \theta & \frac{r}{2} \cos \theta \\ \frac{r}{2} \sin \theta & \frac{r}{2} \sin \theta \end{bmatrix} \begin{bmatrix} \dot{\phi}_r \\ \dot{\phi}_l \end{bmatrix},$$

which gives us a 2×2 matrix. However, it is clear that this matrix is singular, and therefore not invertible. Think about the physical interpretation underlying this observation.

We therefore redefine our Cartesian coordinates to be (x_P, y_P) , the coordinates of a reference point, P , in Figure 5. This point is a distance l away from the axle, along the x axis. The coordinates of the reference point P given by:

$$X_P = \begin{bmatrix} x + l \cos \theta \\ y + l \sin \theta \end{bmatrix} \quad (20)$$

The redefined Cartesian velocities, $\xi = \dot{X}_P$, are given by:

$$\xi = \begin{bmatrix} 1 & 0 & -l \sin \theta \\ 0 & 1 & l \cos \theta \end{bmatrix} \dot{X} = \begin{bmatrix} 1 & 0 & -l \sin \theta \\ 0 & 1 & l \cos \theta \end{bmatrix} \begin{bmatrix} \frac{r}{2} \cos \theta & \frac{r}{2} \cos \theta \\ \frac{r}{2} \sin \theta & \frac{r}{2} \sin \theta \\ -\frac{r}{d} & \frac{r}{d} \end{bmatrix} \dot{q} \quad (21)$$

Multiplying the two matrices gives us the Jacobian matrix:

$$\xi = J \dot{q}, \quad (22)$$

$$J = \begin{bmatrix} \frac{r}{2} \cos \theta + \frac{rl}{d} \sin \theta & \frac{r}{2} \cos \theta - \frac{rl}{d} \sin \theta \\ \frac{r}{2} \sin \theta - \frac{rl}{d} \cos \theta & \frac{r}{2} \sin \theta + \frac{rl}{d} \cos \theta \end{bmatrix}$$

Verify that this matrix is 2×2 and non singular for all values of θ and nonzero values of r , l , and d . J allows us to transform wheel velocities to Cartesian velocities and its inverse maps desired Cartesian velocities into wheel velocities.

5 Control

Desired path and error

We assume that the desired path, \mathcal{C} , is given by an implicit function $\gamma(x, y) = 0$ and the desired speed, v^{des} , is known as a function of the position on the trajectory.

There are two choices for the *path error* [4]:

- Find the point with coordinates (ξ^*, η^*) on the path that is closest to the reference point, P .

$$e(x) = \min_{(\xi, \eta) \in \mathcal{C}} \sqrt{(x_P - \xi)^2 + (y_P - \eta)^2}.$$

This is a hard problem to solve because there are multiple solutions for an arbitrary curve.

- Approximate the distance between the reference point and the curve:

$$e_1(x) = \gamma(x_P, y_P) = \gamma(x + l \cos \theta, y + l \sin \theta).$$

We will use this error metric in the rest of the discussion.

If v^{des} is specified along $\gamma(x, y) = 0$, *i.e.*, $v^{des}(x, y)$ is known, the natural measure for the *speed error* at any point (x, y) is:

$$e_2 = v^{des} - \sqrt{\dot{x}_P^2 + \dot{y}_P^2}.$$

Note that this error does not depend explicitly on the state.

Control law

We want the error dynamics to obey a differential equation that guarantees that the error converges exponentially to zero. We take advantage of the fact that the solution to any homogeneous, first order linear differential equation with positive, constant coefficients is an exponential that converges to zero. For example, the differential equation,

$$y' + ky = 0, \quad (0) = y_0$$

has the solution

$$y(x) = y_0 \exp(-kt).$$

We want the path error to converge exponentially to zero -

$$\dot{e}_1 + k_p e_1 = 0. \tag{23}$$

In other words, we want

$$\begin{aligned} \dot{e}_1 &= \begin{bmatrix} \frac{\partial \gamma}{\partial x_P} & \frac{\partial \gamma}{\partial y_P} \end{bmatrix} \begin{bmatrix} \dot{x}_P \\ \dot{y}_P \end{bmatrix} \\ &= \Gamma J \dot{q} \\ &= -k_p \gamma(y) \end{aligned}$$

where

$$\Gamma = \begin{bmatrix} \frac{\partial \gamma}{\partial x_P} & \frac{\partial \gamma}{\partial y_P} \end{bmatrix}.$$

Or we can write

$$\Gamma J \dot{q} = -k_p \gamma(y(x)) \quad (24)$$

This equation uses the path errors to command motor speeds ensuring that the errors converge to zero. This is an example of a feedback control law — the path error is used as feedback information to guarantee performance.

The speed error e_2 is a function of the input:

$$e_2 = v^{des} - \frac{r}{2}(\dot{\phi}_r + \dot{\phi}_l) = v^{des} - \frac{r}{2} \begin{bmatrix} 1 & 1 \end{bmatrix} \dot{q} \quad (25)$$

So we can drive the error to zero instantaneously by simply computing \dot{q} so that e_2 is zero. But note that this does not allow for any feedback of possible errors and steady state introduced by an inaccurate geometric model or inability to drive perfectly in the real world.

In order to eliminate steady state errors we introduce integral feedback and require the error e_2 to satisfy:

$$e_2 + k_i \int e_2 dt = 0 \quad (26)$$

By differentiating this equation you will see that it reduces to the familiar first order linear differential equation in e_2 which guarantees exponential convergence. From (26), we get

$$\begin{aligned} e_2 &= v^{des} - \frac{r}{2} \begin{bmatrix} 1 & 1 \end{bmatrix} \dot{q} \\ &= -k_i \int e_2 dt \end{aligned}$$

In other words,

$$v^{des} - \begin{bmatrix} 1 & 1 \end{bmatrix} \dot{q} = -k_i \int e_2 dt \quad (27)$$

Taking Equations (24, 27) we have two equations to compute the wheel velocities \dot{q} . Denoting the 1×2 row vector of ones by $\mathbf{1}^T$, we write

$$\begin{bmatrix} \Gamma J \\ \frac{r}{2} \mathbf{1}^T \end{bmatrix} \dot{q} = \begin{bmatrix} -k_p e_1 \\ v^{des} + k_i \int e_2 dt \end{bmatrix} \quad (28)$$

We can verify that the coefficient matrix in front of \dot{q} is non singular for non zero l and can be inverted to find \dot{q} so that Equations (24, 27) are satisfied. The resulting controller requires as feedback the knowledge of the errors, e_1 and e_2 , the integral of the error e_2 , and the state (angle θ) to compute all the terms, in addition to the specification of the path $\gamma(x, y)$ and the speed, $v^{des}(x, y)$, along the path.

References

- [1] S. M. LaValle. *Planning Algorithms*. Cambridge University Press, Cambridge, U.K., 2006. Available at <http://planning.cs.uiuc.edu/>.
- [2] N. Michael, J. Fink, and V. Kumar. Experimental testbed for large multi-robot teams: Verification and validation. 15(1):53–61, March 2008.
- [3] R. Murray, Z. Li, and S. Sastry. *A Mathematical Introduction to Robotic Manipulation*. CRC Press, Florida, 1994.
- [4] N. Sarkar, V. Kumar, and X. Yun and. Control of mechanical systems with rolling contacts: Applications to mobile robots. *International Journal of Robotics Research*, 13(1):55–69, February 1994.
- [5] Benson H. Tongue and Sheri D. Sheppard. *Dynamics: Analysis and Design of Systems in Motion*. John Wiley and Sons, 2005.